Plasma manipulation techniques for positron storage in a multicell trap

J. R. Danielson, T. R. Weber, and C. M. Surko
Department of Physics, University of California, San Diego, 9500 Gilman Drive, La Jolla, California 92093-0319

(Received 28 August 2006; accepted 18 October 2006; published online 4 December 2006)

New plasma manipulation techniques are described that are central to the development of a multicell Penning trap designed to increase positron storage by orders of magnitude (e.g., to particle numbers $N \geqslant 10^{12}$). The experiments are done using test electron plasmas. A technique is described to move plasmas across the confining magnetic field and to deposit them at specific radial and azimuthal positions. Techniques to fill and operate two in-line plasma cells simultaneously, and the use of 1 kV confinement potentials are demonstrated. These experiments establish the capabilities to create, confine, and manipulate plasmas with the parameters required for a multicell trap; namely, particle numbers $>10^{10}$ in a single cell with plasma temperature $\leqslant 0.2$ eV for plasma lengths ~ 10 cm and radii $\leqslant 0.2$ cm. The updated design of a multicell positron trap for 10^{12} particles is described.
 [DOI: 10.1063/1.2390690]

I. INTRODUCTION

Phenomena involving positrons (i.e., the antiparticles of electrons) are important in many fields of science and technology, including astrophysics, plasma and atomic physics, and materials science.[1–6] Scientific applications include Bose-condensed gases of positronium atoms and the formation and study of antihydrogen (i.e., stable, neutral antimatter). Technological applications include the characterization of materials for semiconductor chip manufacture. On a longer time horizon, potential applications include the creation of an annihilation gamma-ray laser.[7]

Many of these applications require large numbers of positrons and/or long storage times or would benefit by the development of portable antimatter traps. A major impediment to pursuing these goals has been the inability to efficiently accumulate, cool, manipulate, and store large numbers of low-energy positrons. There has been continued progress in this area over the last decade using the basic experimental technique of positron confinement in Penning-Malmberg traps, such as that illustrated in Fig. 1. This device uses a uniform magnetic field and cylindrical electrodes with electrostatic potentials on the ends to confine the particles (e.g., positrons, electrons, ions, or antiprotons).[2,8–10] While the principal objective is the accumulation, manipulation and storage of positrons (i.e., antimatter), the work reported in this paper and much previous work in this area uses conventional single-component electron plasmas for increased data rate and ease of handling. In an actual positron application, a conventional electron source would be replaced by bursts of positrons that are now accumulated routinely and efficiently using the buffer-gas trapping technique.[2,11,12]

Progress over the past two decades in accumulating large numbers of positrons is illustrated in Fig. 2. The work reported here takes the next steps in this research. The goal is to increase by orders of magnitude the number of positrons (presently $N \sim 10^9$) that can be accumulated and stored for long periods. Impediments to further progress are dealing with large values of plasma space charge and achieving very long confinement times (e.g., days) for high-density positron plasmas. Small positron plasmas ($N < 10^4$) have been confined at high densities ($n > 10^9$ cm^{-3}) for several weeks in a laser-cooled ion plasma.[13] No experiments to date have demonstrated the long-term confinement of large numbers of particles.

Recently, a novel design for a *multicell* Penning-Malmberg trap was proposed to achieve these objectives.[14,15] Note that here and elsewhere in this paper, we refer to a "cell" as a single-component plasma in an individual Penning-Malmberg trap in the case in which more than one such plasma is arranged in the same magnetic field and vacuum system. This multicell design confines the stored antiparticles in numerous, separate plasma cells shielded from one another by copper electrodes. These electrodes screen out the plasma space charge, reducing the required confinement voltages by an order of magnitude or more. This multicell design, using relatively short plasmas and small values of space charge potential, improves plasma confinement and reduces plasma heating and the requirements for electrode and magnetic field uniformity. We note that multicell traps have also been developed for other applications; namely, arrays of quadrupole mass spectrometers used to increase sample analysis throughput.[16,17]

The specific objective that motivates the present experiments is development of the technology required to build a 95-cell Penning-Malmberg trap in a common magnetic field and vacuum system that can store $\geqslant 10^{12}$ positrons for weeks without significant loss. As illustrated in Fig. 2, this would increase the present state of the art by a factor $\sim 10^3$. Such a device would also represent a major step toward the development of a versatile, *portable* antimatter trap—decoupling the end use of the antimatter from the need for a fixed, intense source of antiparticles such as particle accelerator or radioactive materials. Described here are key techniques that will enable the building of a practical multicell positron trap.

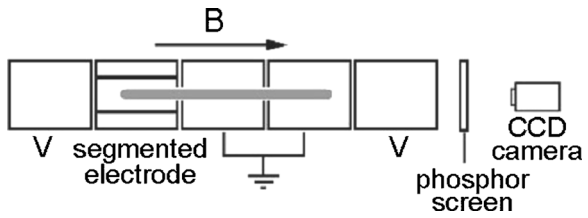

FIG. 1. Schematic diagram of a Penning-Malmberg trap. As shown, it consists of five cylindrical electrodes, including one that is segmented azimuthally for radial plasma compression and the excitation of plasma modes. Also shown is a phosphor screen and CCD camera that are used to image radial density profiles of confined plasmas. The actual device used for the experiments reported here is illustrated in more detail in Fig. 4 below.

In particular, techniques are demonstrated to handle large values of space charge, to operate two in-line plasma cells, and to fill off-axis cells.

II. THE MULTICELL POSITRON TRAP CONCEPT

The concept of the multicell Penning-Malmberg trap is shown schematically in Fig. 3.[14] There are several potential factors limiting long-term confinement of large numbers of positrons in Penning-Malmberg traps. One such consideration is the Brillouin limit, which is the limiting density for plasma confinement in a uniform magnetic field. For electrons or positrons at tesla-strength magnetic fields, the Brillouin limit is beyond the capability of present-day experimental capabilities, so that it is not of immediate concern. A more severe limitation is the effect of plasma space charge, which is an important practical constraint in present-day positron traps. For large particle numbers N, the space charge potential of a cylindrical, single-component plasma of length L in a Penning-Malmberg trap is proportional to N/L. For fixed plasma length L, the number of particles N that can be stored in a trap is limited by the maximum potential, V_C that can be applied to electrodes (i.e., in vacuum, in the presence of the plasma). For a long, uniform plasma of radius R_p in a cylindrical electrode structure of radius R_w, the on-axis space charge potential ϕ_o (in volts) is

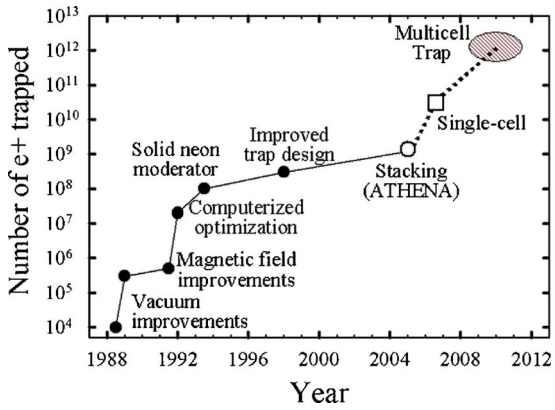

FIG. 2. (Color online) (●) progress in positron trapping from similar strength sources (~50–100 mCi ^{22}Na) using a buffer-gas accumulator (Refs. 2, 11, 12, and 20) including (○) stacking positron plasmas in UHV (Ref. 20). Dashed line indicates projected results: (□) parameters achieved here for an electron plasma, and (oval) the expected value for the 95-cell multicell trap described here.

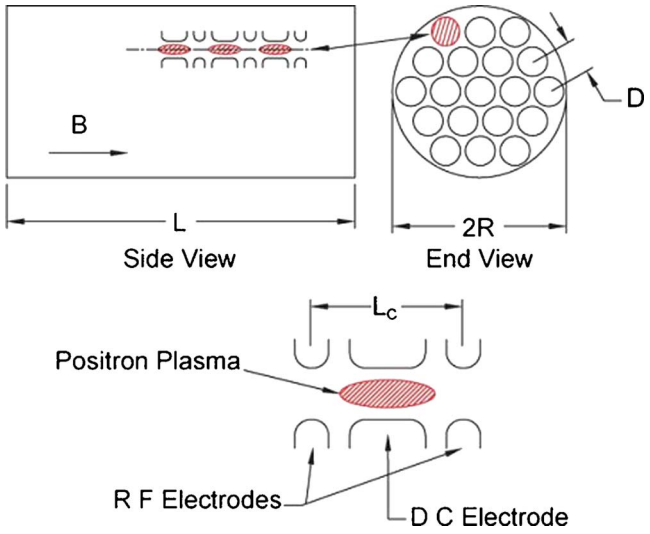

FIG. 3. (Color online) Conceptual design of a 95-cell trap, showing the arrangement of cells parallel and perpendicular to B. This device consists of 19 hcp cells perpendicular to the magnetic field and five in-line cells in the field direction. The design parameters for this device are summarized in Table I.

$$\phi_o = 1.4 \times 10^{-7}(N/L_p)[1 + 2\ln(R_w/R_p)], \quad (1)$$

where L_p is in centimeters. From Eq. (1), for example, for a plasma of 10^{10} positrons with $L_p = 10$ cm and $R_w/R_p = 8.8$, $\phi_o = 750$ V, which in turn, requires a value of $V_C > 750$ V. In principle, one could envision using very large values of V_C. However, the maximum possible operating potential for a compact Penning-Malmberg trap, with closely spaced electrodes used to confine large numbers of electron-mass particles in a strong magnetic field, depends upon the specifics of the apparatus and must be demonstrated experimentally.

Another consideration arises from the fact that heating (i.e., due to outward diffusion) is proportional to the space charge potential ϕ_o.[14] This heating can inhibit the ability to confine and compress positron plasmas. It can also lead to positronium formation on background impurities in the vacuum system, and this represents a potentially serious positron loss process. This process, which has a positron-energy threshold of a few electron volts and a large cross section, i.e., $\sim 10^{-16}$ cm^2, involves a positron capturing an electron from a background impurity atom in the vacuum system. The resulting neutral Ps atom will then quickly annihilate. To avoid this loss, stored positron plasmas must be kept relatively cool (e.g., $T \leqslant 1$ eV), and thus unnecessary plasma heating must be avoided.

A key feature of the multicell trap is that the effect of large values of space charge potential is mitigated by dividing the plasma into m rod-shaped plasmas of length L, each oriented along the magnetic field [e.g., in a hexagonal-close-packed (hcp) arrangement transverse to the field]. These rod-shaped plasmas are shielded from each other by close-fitting copper electrodes. For a given maximum confining electrical potential, V_C, applied to the electrodes, the number of stored positrons will be increased by a factor of m. Since the plasma heating rate due to outward expansion of the plasma is proportional to the plasma space charge, the multicell design

TABLE I. Design parameters of a multicell trap for 10^{12} positrons.

Number of cells ($m \times p = 19 \times 5$)	95
Total positron number N (10^{12})	>1
Positrons per cell N_C (10^{10})	>1
Magnetic field (T)	5
Electrode length L (cm)	65
Electrode diameter $2R$ (cm)	8.5
Confinement voltage V_c (kV)	1.0
Cell dimensions D (cm)	1.7
L_c	10
R_w	0.6
Plasma dimensions R_p (cm)	0.13
L_P	8
Plasma density (10^{10} cm^{-3})	2.5
Plasma temperature (eV)	0.1
Space charge potential (V)	700
Rotating wall frequency (MHz)	8

also reduces the requirements on plasma cooling. In the trap design considered here, cooling is accomplished by cyclotron radiation of the particles in a relatively large (e.g., several tesla) magnetic field.

The multicell design also breaks up each long rod of plasma into p separate plasmas in the direction along the magnetic field (i.e., separated by electrodes at potential V_c). The plasma length is decreased by a factor L/p. This reduces the effects of (off-axis) magnetic nonuniformities. It also reduces the rate of outward, asymmetry-driven radial transport (i.e., which is typically found to be proportional to L^2[18]) during the filling and compression cycles. The proposed design parameters for a 95-cell multicell trap are summarized in Table I. The electrode structure will be cooled to cryogenic temperatures to ensure an ultrahigh vacuum (UHV) environment. Positron loss is expected to be small on the design-goal time scale of weeks. As indicated in Table I, the plasma is expected to be considerably warmer than the electrode temperature (i.e., ~0.1 eV) due to plasma heating from the radio frequency fields used to achieve long-term plasma confinement.

The work reported here used a confinement potential $V_C = 1.0$ kV, which resulted in a maximum particle number of $N = 3 \times 10^{10}$ in a single Penning-Malmberg cell. The design in Table I is likely conservative in this regard. If one could work with ~3 kV, which is likely, a trap for 10^{12} positrons would require only 24 cells. Alternatively, a 95-cell trap could confine 3×10^{12} positrons.

Positrons to fill the multicell trap will be accumulated in a specially designed buffer-gas Penning-Malmberg trap.[12] Positron plasmas in the buffer-gas trap cool to room temperature in ≤0.1 s due to collisions with the buffer gas. The trapping efficiency of 25% is more than an order of magnitude larger than any other technique developed to date. Typically $N \sim 3 \times 10^8$ e^+ can be accumulated from a 100 mCi ^{22}Na radioactive source and noble gas moderator in a few minutes. Positron plasmas from the buffer-gas trap will be "stacked"[19–21] in UHV in the high-field trap[20] on a several minute cycle time to achieve ≥10^{10} positrons in a single plasma cell. At these fill rates, trapping 10^{12} positrons would take several days to a week. However, stronger positron sources are currently in operation and/or under development in a number of laboratories around the world that could fill such a trap in a few hours or less.[2,22–24]

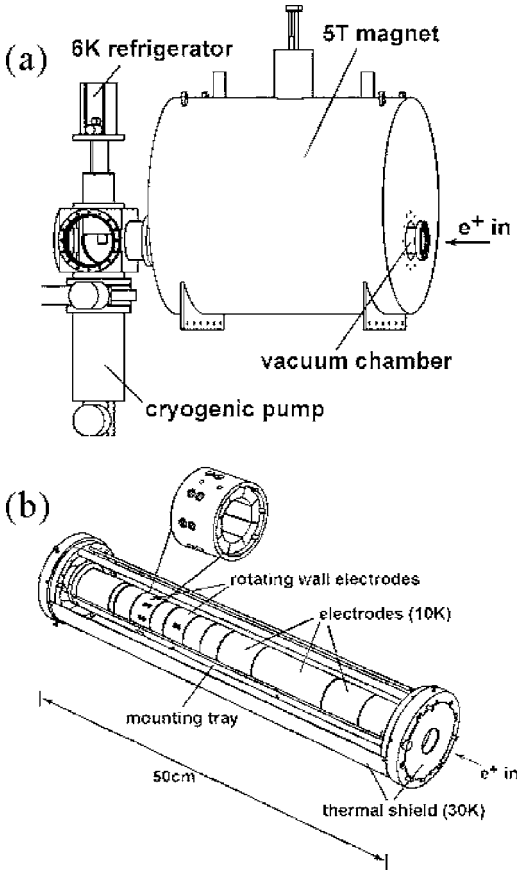

FIG. 4. (a) Overview of the high-field trap apparatus. (b) Electrode structure used for the experiments reported here.

As described in Sec. IV C below, a new feature has been added to the design, namely, a master plasma manipulation cell, the purpose of which is to receive plasmas from the buffer gas trap, compress them, and move them off axis radially before depositing them in the multiple storage cells. The design in Table I includes an additional 15 cm of electrode length for this master cell.

III. DESCRIPTION OF THE EXPERIMENTS

Experiments were performed in the cylindrical Penning-Malmberg trap, shown schematically in Fig. 4. This device has been described in detail previously;[15,25,26] thus, here we review only briefly key features of the apparatus. While the device has the capability to cool the electrode structure to cryogenic temperatures, the experiments reported here were done with the electrodes at 300 K. Plasmas can be confined in various combinations of cylindrical electrodes ($R_w = 1.27$ cm) to achieve plasma lengths in the range $5 \leq L_p \leq 25$ cm. Two of the electrodes are segmented (one with eight sectors and another with four sectors) in the azimuthal direction. Electron plasmas are injected using a standard electron gun and are confined radially by an applied 5 T

TABLE II. Summary of plasma parameters achieved for a 1000 V confinement potential, including the confinement length L_c, fill voltage V_f, total particle number N, plasma radius R_p, plasma length L_p, plasma density $\bar{n}$, and the space charge potential ϕ_o.

L_c (cm)	V_f (V)	N (10^{10})	R_p (cm)	L_p (cm)	$\bar{n}$ (cm^{-3})	ϕ_0 (V)
	300	0.18	0.18	4.7	0.38	270
5.08	600	0.42	0.10	5.5	2.4	670
	900	0.70	0.07	7.3	6.2	930
	300	0.42	0.18	9.8	0.42	300
10.2	600	0.91	0.11	10.8	2.2	715
	900	1.60	0.09	14.7	4.3	990
	300	0.90	0.18	20.0	0.44	320
20.3	600	1.90	0.19	20.6	0.81	640
	900	3.30	0.19	23.4	1.2	975

magnetic field, with axial confinement provided by voltages applied to the end electrodes. In typical experiments, rotating electric fields could be applied to compress the plasmas and achieve long-term confinement [i.e., the so-called "rotating wall" (RW) technique]. This was accomplished using a special-purpose, four-phase rf generator attached to the four-sector electrode to produce a radial electric field with azimuthal mode number $m_\theta=1$ rotating in the same direction as the plasma. The segmented electrodes were also used to excite and detect diocotron modes in the plasma that, as described below, were used to move plasmas across the magnetic field.

The trap is operated in "inject-manipulate-dump" cycles that exhibit very good shot-to-shot reproducibility. Dumped electron plasmas are accelerated to about +5 kV before striking a phosphor screen, with the resulting images recorded by a CCD) camera. This z-integrated profile and the trap geometry are used to calculate the plasma length and plasma density using a Poisson-Boltzmann code. Typical values of plasma space charge ϕ_0 ranged from 10 to 990 V. The parallel plasma temperature $T_\parallel$ was measured by slowly lowering the confinement voltage and measuring the escaping charge.[27]

The plasma is cooled by cyclotron radiation in the 5 T magnetic field at a rate $\Gamma_c=(1/T)(dT/dt)\sim 6\ \mathrm{s}^{-1}$,[28] which is fast compared to the compression and expansion rates. Steady-state plasmas were found to remain relatively cool (i.e., $T\leqslant 0.2$ eV; $T/e\phi_0\ll 1$), even in the presence of strong RW fields.

After the plasma is injected into the trap, the RW field was turned on with amplitude V_{RW} and frequency f_{RW}. The evolution of the plasma was studied by repeating the experiment for different hold times. The plasma reaches a steady state after a few seconds.[25,26] Experiments on longer time scales have shown that this steady-state density *can be maintained for more than 24 h* with no loss of plasma. Initially, in steady state, and in expansion after the RW is turned off, the plasma profiles are close to that of a rigid rotor (i.e., constant density), except slightly broadened at larger radii.

IV. EXPERIMENTAL RESULTS

In this section, we describe the results of experiments to establish techniques critical to the development of a multicell trap. In particular, we demonstrate the ability to operate with kilovolt electrical potentials and to operate two in-line plasma cells simultaneously. We also describe a new technique to move plasmas across the magnetic field and deposit them at specific radial and azimuthal locations. This latter technique will be used to fill off-axis plasma cells.

A. Operation with kilovolt confinement potentials

While plasmas have been confined previously in Penning-Malmberg traps with kilovolt potentials (e.g., see Refs. 29–31), it is important to establish this capability in specific situations with electrode spacings relevant to the multicell trap. Special programmable power supplies were designed and built to operate at kilovolt confinement potentials. Plasmas were created and confined using a 1.0 kV confinement potential for three different confinement lengths: $L_c=5.1$, 10.2, and 20.3 cm. Data for these lengths and three fill voltages are summarized in Table II. The maximum space charge potential ϕ_0 was 990 V for $V_c=1000$ V. This represents a net excess confinement potential of only 10 V, which is made possible by the low values of plasma temperature; i.e., $T\leqslant 0.5$ eV. Note that the plasma length self-adjusts to some extent, depending upon the value of ϕ_0 relative to V_c, and the ratio, R_w/R_p. In these experiments, plasma radii were set by the characteristics of the electron gun and the filling procedure as opposed to using plasma expansion and/or rotating wall compression to adjust R_p. The maximum plasma density achieved was 6.2×10^{10} cm^{-3}.

The dependence of plasma density on the total number of particles N is illustrated in Fig. 5(a) for the three different confinement lengths (L_c). The dependence of N on L_c for the three different filling voltages (V_f) is illustrated in Fig. 5(b). Several of the cases exceed the $N=1\times 10^{10}$ particle design goal. The closest case to the nominal parameters in Table II is $L_c=10.2$ cm and $V_f=600$ V. The parameters for this case could be made to match very closely the design parameters by adjusting the plasma density and radius using the rotating wall compression.

B. Simultaneous operation of two plasma cells

The ability to create and manipulate two, in-line plasmas was investigated. This experiment is illustrated in Fig. 6. Plasmas were loaded in two separate cells of the high-field trap using a "fill-shuttle-fill-hold" protocol. Following the

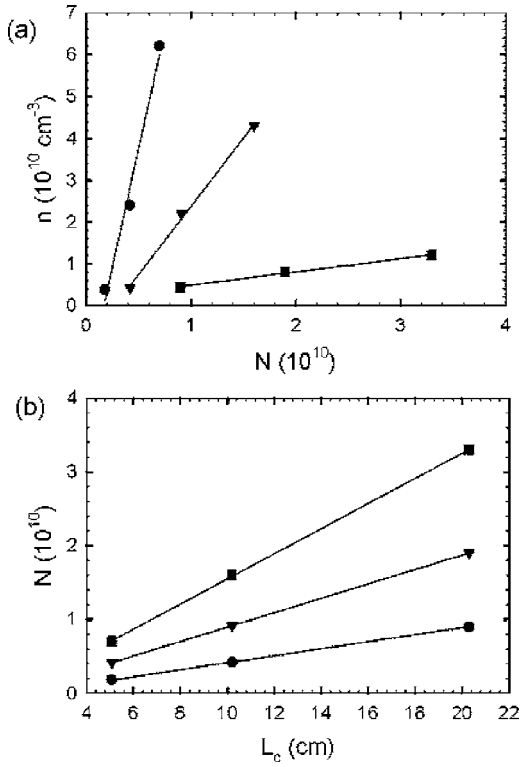

FIG. 5. (a) The dependence of plasma density on total number N for three different confinement lengths L_c of (●) 5.1, (▼) 10.2, and (■) 20.3 cm. (b) The dependence of N on L_c for three different fill voltages: V_f: (●) 300, (▼) 600, and (■) 900 V. For all experiments, the confinement voltage V_c=1.0 kV.

"hold" stage, independent control of the plasmas was demonstrated by depositing them sequentially onto the phosphor screen where each could be imaged separately. Each plasma consisted of $N \approx 5.5 \times 10^8$ electrons. The plasmas were 10 cm long, 0.93 mm in radius, and were separated axially by 10 cm. It was confirmed that there was no increase in outward radial transport with the addition of the second plasma to the trap. The plasmas were confined for 30 s with no noticeable expansion. Additional studies will be required to investigate confinement of these multicell, trapped plasmas at higher densities and on longer time scales.

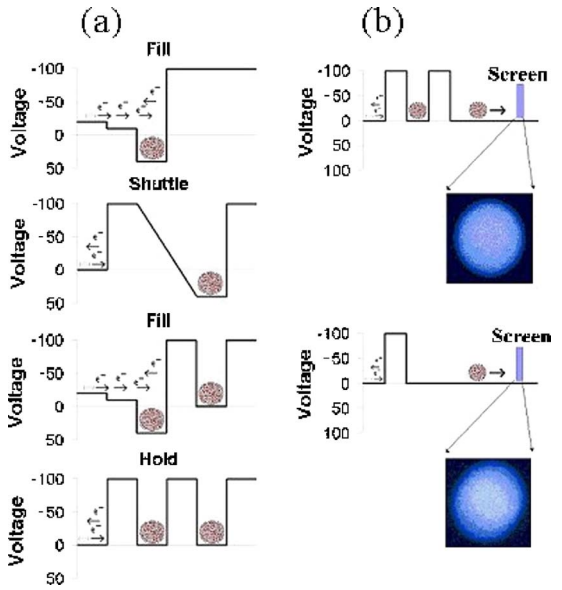

FIG. 6. (Color online) Schematic diagram of (a) the potential profile during the sequential filling of two in-line plasma cells with electron plasma and (b) the sequential dumping of these plasmas and the resulting images.

C. Moving plasma across the magnetic field

One of the key requirements for a multicell trap is development of a robust and compact method to move plasma across a magnetic field. While this could be accomplished by magnetic deflection or use of $\boldsymbol{E}\times\boldsymbol{B}$ plates, both techniques have disadvantages in terms of space requirements and the need to switch large magnetic fields and/or electrical potentials. To solve this problem, we developed a novel method that involves excitation of a so-called "diocotron" mode of the plasma.[18] Specifically, when a single-component plasma is displaced from the axis of the cylindrical electrode, the center of mass will $\boldsymbol{E}\times\boldsymbol{B}$ drift in the field of the image charge of the plasma. This drift of the plasma about the axis is known as a diocotron mode. The amplitude of this mode is the displacement D of the plasma from the axis of symmetry of the confining electrodes.

For a long plasma column with $L_p \gg R_w$, the linear frequency of the $m_\theta=1$, $k_z=0$ diocotron mode is approximately $f_D \approx (R_p/R_w)^2 f_E$, where f_E is the plasma $\mathbf{E}\times\mathbf{B}$ rotation frequency, $f_E = cne/B$, where c is the light speed and B the magnetic field strength.[31] For the work reported here, the plasmas were typically quite narrow, with $R_p \ll R_w$, and $f_D \sim$ a few kHz $\ll f_E$. The diocotron mode was excited by applying a sinusoidal signal at a frequency near f_D to one sector of the four-sector electrode using the technique of "autoresonance." As described below, this technique provides an effective and convenient method to control both the amplitude (i.e., radial displacement D) and the azimuthal position of the plasma column as a function of time.

The frequency and amplitude of the diocotron mode were measured, independent of the excitation, on a separate sector of the segmented electrode. By exciting the diocotron mode to different amplitudes, we obtain plasmas at different displacements from the trap axis. However, for large displacements, the gradient of the induced electric field across the plasma increases and the plasma distorts, producing a nonlinear shift in the mode frequency. To lowest order, and assuming $R_p \ll R_w$, this nonlinear frequency can be written as

$$f_{\mathrm{NL}} \approx f_D \frac{1}{1-(D/R_w)^2}, \tag{2}$$

where f_D is the linear diocotron mode frequency.[32] Figure 7 shows the measured nonlinear diocotron frequency normalized to the linear frequency for excitations up to $D/R_w \sim 0.8$. Equation (2) is plotted as the black line with no adjustable parameters.

To measure the mode amplitude non-perturbatively, the received signal was amplified and fed into a spectrum analyzer. The finite angular extent of the receiver electrode (90°), means that the received signal is composed of the fundamental frequency and its harmonics, $f_n = n f_{\mathrm{NL}}$.[33] The

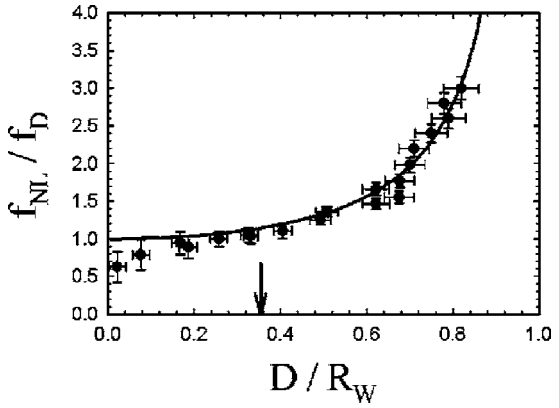

FIG. 7. The diocotron frequency (●) measured for plasmas displaced different distances D from the electrode center; (—) the prediction of Eq. (2) with no fitted parameters. The linear diocotron frequency is f_D=2.9 kHz. The arrow marks the maximum displacement measurable on the phosphor screen.

amplitudes of these harmonics are related to the plasma displacement D by $V_n=A_nD^n$, where the A_n are known coefficients related to the receiver electrode dimensions and the electrical circuit impedance. The displacement D is proportional to V_1 (i.e., the amplitude of the fundamental frequency component of the signal); namely, $D=V_1/A_1$. However, in practice, the expression $D=(A_1/A_2)(V_2/V_1)$, was used to measure D, since this expression is independent of receiver-amplifier gain.[33,34] Figure 8 shows the displacement, as measured using the ratio V_2/V_1, for different excitation levels V_1 for the data set in Fig. 7.

Plasmas can also be imaged directly with the CCD camera out to a displacement $D\approx 0.45$ cm, which provides a direct measurement of this quantity. These values are also plotted in Fig. 8. There is very good agreement (i.e., $\leqslant \pm 10\%$ difference) between the two sets of measurements in the region of overlap of the two techniques. This confirms the ability to create large displacements and detect them using measurements of the frequency harmonics of the excited diocotron mode. The circled point in Fig. 8 represents a displacement to 80% of the electrode radius. This has important, positive, implications concerning the ability to completely fill an electrode structure with multicell plasmas.

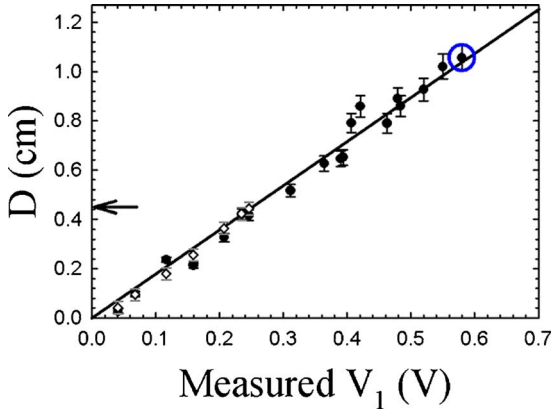

FIG. 8. (●) Displacement D from measurement of the harmonic ratio V_2/V_1, plotted as a function of V_1. Also shown (◇) are the displacements measured directly from images on the phosphor screen. The arrow marks the maximum displacement measurable on the phosphor screen. The circled point corresponds to a displacement of 1 cm, which is 80% of the wall radius.

Knowing the mode frequency, amplitude, and phase relative to one of the sectors, the plasma can be dumped at any location by phase locking to the received mode signal. However, the nonlinear frequency shift makes it difficult to phase lock at arbitrary mode amplitude (i.e., plasma displacement). As mentioned above, this problem was solved using a nonlinear phase locking technique called "autoresonance," which is the tendency of a weakly driven nonlinear system to stay in resonance with the drive signal even when the system parameters vary.[35–37] Using this technique, by varying the drive frequency, one can control the mode frequency and thus control the displacement of the plasma column.

In the work reported here, as in Ref. 36, the diocotron mode is brought into autoresonance by sweeping the drive frequency from below the linear diocotron frequency to a selected, higher frequency. If the drive voltage is sufficiently strong, the excited diocotron mode amplitude (i.e., the displacement D of the plasma column) will grow as the mode increases in frequency to match that of the drive. In this autoresonant condition, the excited diocotron mode will stay phase-locked to the applied signal for as long as the excitation is applied, limited only by plasma expansion. This matching of frequencies and phase occurs for only a limited range of applied amplitudes and sweep rates. If the drive voltage is too small, the mode is not excited; if the drive voltage is too large, higher-order nonlinear effects dominate and destroy the autoresonance. Further, if the sweep rate is too fast, then there is insufficient time for the mode to lock to the drive. These details have been discussed in a series of papers by Fajans *et al.*[35–37] In the work presented here, we explore several unique features of autoresonant diocotron excitation. As shown in Figs. 7 and 8, we demonstrate that large amplitude diocotron modes can be used very effectively to achieve off-axis plasma states. Specifically, we have created radial plasma displacements much larger than the plasma radius (e.g., $D\sim 10R_p$), and as large as 80% of the wall radius. We also demonstrate by direct imaging that phase-locked plasma states can be achieved at arbitrary plasma displacements. Finally, we demonstrate that, by controlled dumping of off-axis plasmas, these techniques could be used to inject plasma into the off-axis cells of a multicell trap.

Figure 9 shows a model calculation of the autoresonant response of a small plasma to a constant-amplitude sine wave, i.e., $V_D=V_o\sin(2\pi ft)$, as the frequency f of the applied sine wave is changed. The initial on-axis plasma is driven to a large displacement when the frequency of the drive is swept from below the linear mode frequency to a higher frequency. The final displacement D is determined by the final frequency of the applied signal, and the phase angle in the plane perpendicular to the cylindrical axis is determined by the phase of this applied signal. After autoresonance has been achieved, the plasma will stay locked, both in phase and frequency (and hence displacement), for thousands

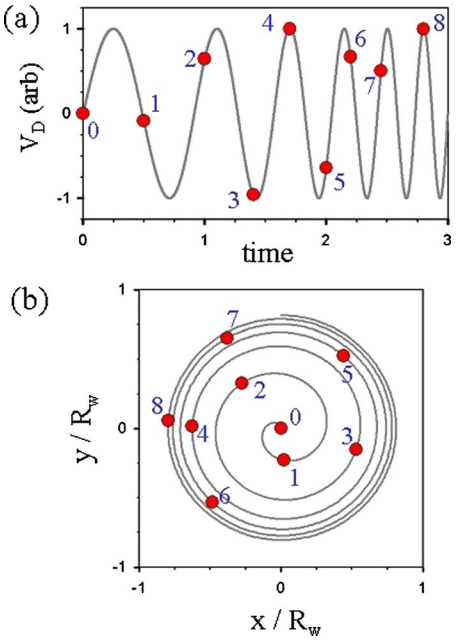

FIG. 9. (Color online) Model calculation of the evolution of plasma position during the excitation of a nonlinear diocotron mode: (a) the drive voltage $V_D(t)$ and (b) corresponding plasma orbit in the (x,y) plane perpendicular to the magnetic field. Numbers correlate position with the phase of the drive signal. In (a), time is in units of the period, τ_1, of the linear diocotron mode. As the frequency increases, the plasma column moves to larger displacement.

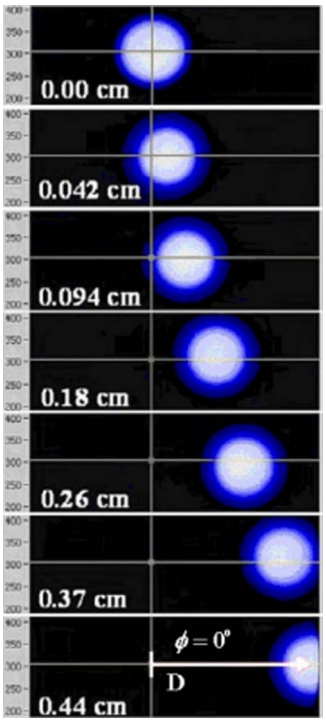

FIG. 10. (Color online) Plasma images for different values of the diocotron drive frequency thus producing different radial displacements D. All plasmas are dumped with phase $\phi=0°$. Note that the plasma extent and shape remains approximately the same, independent of D. These values of D and the values of V_1 to which they correspond are shown as the open diamonds in Fig. 8.

of diocotron periods. The possibility that plasma expansion may limit the utility of the technique at very large times is currently under current investigation.

This technique for moving plasmas to specific positions in the plane perpendicular to the magnetic field was verified in a series of experiments. Plasmas were excited by applying a swept-frequency signal from an arbitrary waveform generator to one segment of the segmented electrode. This signal, initially at some frequency $f_1=1/\tau_1$, chosen to be below the linear diocotron frequency, is increased from zero amplitude to a specified value in $20\tau_1$; then swept up in frequency to $3f_1$ (i.e., chosen to be above the *linear* diocotron frequency) in $20\tau_1$. The plasma is then held at $3f_1$ for $20\tau_1$, before being dumped. In this procedure, the frequency sweep from f_1 to $3f_1$ guarantees that the plasma will under go some nonzero radial displacement D, the value of which is set by the final frequency, $3f_1$. The radial position and profiles of the plasmas were measured using a CCD camera after the plasma particles were accelerated to 8 kV and deposited on the phosphor screen. In a multicell trap, plasmas would be deposited in off-axis cells instead of being dumped onto the phosphor screen.

Figure 10 shows images of autoresonantly excited plasmas that have been deposited on the screen at a fixed phase, i.e., $\phi=0°$, with respect to the drive. For each successive image, the initial frequency f_1 (and hence the final frequency $3f_1$) is increased, resulting in successively larger displacements D, as shown. For these experiments, the maximum viewable displacement on the screen is 0.45 cm, while the wall is at radius $R_w=1.27$ cm. Note that, using this technique, we can obtain displacements that are much larger than the plasma radius; i.e., $D \gg R_p$.

The ability of this technique to deposit plasmas at predetermined *azimuthal* locations was also tested. Figure 11 shows the CCD images when the phase of the excitation corresponds to $\phi=0°$, 90°, 180°, 270°, all at a fixed displacement $D \approx 0.26$ cm. Test experiments to date were limited to these values of the phase. In progress is the development of electronics and software to deposit plasmas at *arbitrary* azimuthal phase angles. Combined with the amplitude control

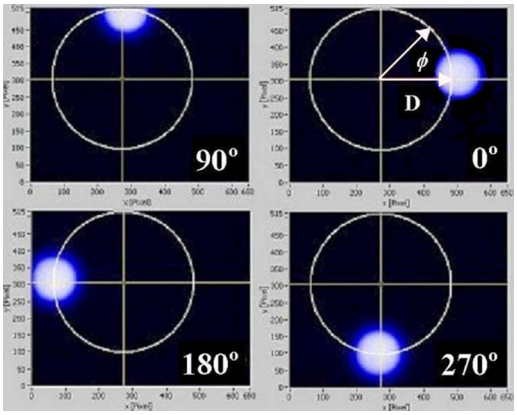

FIG. 11. (Color online) Plasma images for different phase angles ϕ, for $D=0.26$ cm. The image at $\phi=90°$ is clipped due to the limited extent of the phosphor screen.

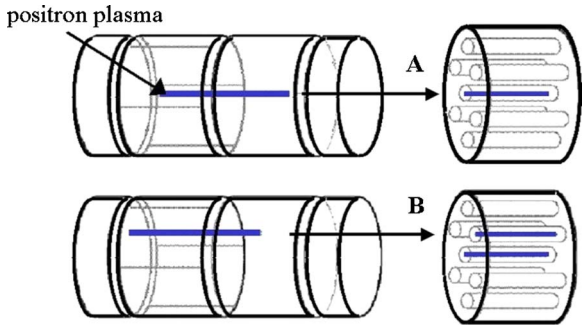

FIG. 12. (Color online) Illustration of use of the autoresonant diocotron-mode technique to inject positrons into specific cells in a "multicell" trap: (left) master plasma manipulation cell, and (right) adjacent bank of multiple cells. In (A), the central cell is filled. In (B), an $m_\theta=1$, $k_z=0$ diocotron mode is excited, then the plasma is injected into the desired line of cells in the multicell trap using gate switching and a fast dump.

described above, this will enable dumping plasmas at arbitrary locations in the plane perpendicular to the magnetic field. The results of the experiments reported here, including the clear, sharp images shown in Figs. 10 and 11, indicate that plasmas can be deposited in specific off-axis cells to a high degree of accuracy (e.g., ±0.2 mm in the radial and azimuthal directions). It should also be noted that plasmas were moved across the magnetic field relatively quickly (e.g., in a few milliseconds). With appropriate choice of the initial value of f_D and careful tuning, it is likely that this time can be considerably reduced.

Figure 12 illustrates how this autoresonant diocotron-mode excitation technique could be used to fill a multicell positron trap. Plasmas from a buffer-gas positron accumulator will be shuttled into a master plasma manipulation cell (Fig. 12, left), then excited to the appropriate values of D and ϕ before being deposited into a specific off-axis cell. Shown in Fig. 13 is a schematic illustration of the design of an electrode structure for a 95-cell trap (i.e., compatible with the design parameters summarized in Table I) incorporating a master plasma manipulation cell for injection into off-axis cells. Each cell has a segmented electrode, an equal-length dc electrode, and confinement electrodes at each end.

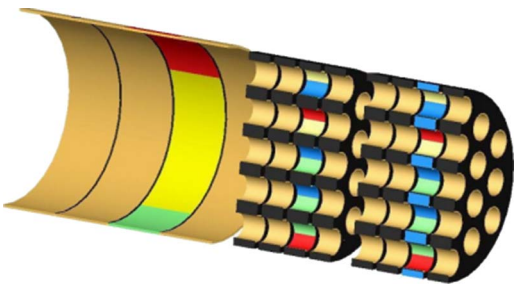

FIG. 13. (Color online) An electrode design for a multicell trap: (left) master plasma manipulation cell; and (right), two blocks of 19 cells in an hcp arrangement. In a 95-cell trap, three more 19-cell blocks would be added at the right.

V. COMPLEMENTARY DEVELOPMENTS

There have been other recent complementary developments that can simplify operation of a practical multicell trap. It is envisioned that the so-called rotating wall (RW) technique will be used to compress single-component plasmas and to achieve essentially "infinite" confinement times. This technique uses an electric field, rotating in the plane perpendicular to the magnetic field, to inject angular momentum into the plasma and compress it radially.[25,26] As originally developed,[18,38,39] this technique required careful tuning to a mode in the plasma to compress weakly coupled plasmas (i.e., plasmas without crystalline ordering) that are relevant here. Recently, a new "strong drive" regime of operation of the rotating wall technique was discovered that does not require tuning to a mode.[25,26] It works over a broad range of frequencies and compresses the plasma until the $\boldsymbol{E}\times\boldsymbol{B}$ rotation frequency f_E equals the applied rotating wall frequency f_{RW}. The final density can thus be controlled by changing the frequency of the applied RW signal and does not depend critically on the RW amplitude. Furthermore, plasmas with a remarkably broad range of initial densities (e.g., varying by a factor of 20 or more) can be compressed or expanded to a given final state density by the application of a single, fixed RW frequency.

This new regime of RW operation is expected to lead to considerable simplifications in the design of a practical multicell trap in that, in this regime of RW operation, active control and interrogation of individual plasma cells is unnecessary. Very recently, much progress has also been made in understanding the coupling of the RW fields to the plasma and the nature of the RW torque to the extent that quantitative predictions can be made for the magnitude of the torque that are in agreement with experiment.[40,41] This aids greatly in being able to make accurate designs for advanced traps for long-term positron storage.

Being able to operate the RW in this strong drive regime also has important consequences in reducing plasma heating. Early multicell designs considered only weak drive operation, where practical considerations for a multicell trap required a RW frequency that was an order of magnitude greater than the plasma $\boldsymbol{E}\times\boldsymbol{B}$ rotation frequency.[14] The resulting "slip" between the RW and the plasma causes excess heating. This can be understood by noting that the minimum heating rate during plasma compression is the rate of conversion of electrostatic energy into heat. This rate is proportional to the $\boldsymbol{E}\times\boldsymbol{B}$ rotation frequency. In contrast, the rate of energy input due to the RW fields is proportional to the (larger) RW frequency.[42,43] Using the RW technique in the strong drive regime, the plasma rotation frequency is quite close to the RW frequency, hence the slip is negligibly small. Thus operation in the strong drive regime approximates closely the minimum possible heating rate—as much as an order of magnitude less heating than in the weak-drive regime.

Furthermore, operating in the strong drive regime, it is possible to access plasma parameters (i.e., for $n\geqslant 6\times 10^9$ cm^{-3} at $B=5$ T), such that the outward transport rate Γ_o, is independent of plasma density (i.e., instead of increas-

ing as $\Gamma_o \propto n^2$, which is the case at lower plasma densities[25,26]). This reduces the required RW drive torque and leads to considerably less plasma heating, so that the plasmas remain cool. Plasmas with parameters such as those listed in Table I can be created with $T \sim 0.1$ eV. This is ideal for the multicell positron trap. In particular, one important consideration is keeping the plasma temperature sufficiently low so that one can avoid positronium formation by collisions of positrons (on the tail of the positron energy distribution) with background impurities present in the vacuum system. The relatively low values of plasma temperature reported here, namely, $T \leqslant 0.5$ eV, fulfill this requirement.

VI. SUMMARY AND CONCLUDING REMARKS

In this paper, we demonstrate techniques critical to the development of a practical, multicell positron trap. Specifically, we demonstrate the ability to operate two plasma cells simultaneously. Off-axis diocotron-mode excitation of plasmas to a displacement 80% of the electrode radius and phased dumping of these off-axis plasmas were demonstrated with a precision that exceeds that required for a practical positron trap. In such a multicell trap, positrons from a buffer-gas accumulator would be shuttled into a master plasma manipulation cell where the positron plasmas would be compressed radially, then deposited in off-axis storage cells through use of the autoresonant diocotron-mode technique. Operation of the trap at confinement potentials of 1 kV was also demonstrated, resulting in the ability to store $\geqslant 10^{10}$ particles in a single cell. In other recent work, it has been shown that plasmas can be compressed radially and maintained for days using the rotating wall compression in the newly discovered strong-drive regime by application of a single, fixed RW frequency, thereby eliminating the need for active control of individual cells of a multicell trap. These results validate key aspects of the design of the multicell positron trap for $N \geqslant 10^{12}$ positrons. Further multiplexing can potentially increase trap capacity by additional orders of magnitude beyond this benchmark goal.

The availability of such large numbers of positrons opens up many new possibilities, such as providing bursts of positrons far larger than available by any other means. Applications of large pulses of positrons include enabling improved methods to create low-energy antihydrogen and Bose-condensed gases of positronium atoms (i.e., the first step toward a gamma-ray laser) and study of electron-positron plasmas.

The successful development of such a multicell trap will also be a major step toward the creation of a versatile *portable* antimatter trap. While portable traps have been discussed previously,[2,44,45] none have yet been developed. Such portable traps can be expected to be important for the many applications, such as those in which radioactive and/or accelerator-based positron sources present significant difficulties (e.g., radiation licensing requirements and radiation shielding). These applications include use of positrons for the characterization of materials for electronic chip manufacture and operations in a satellite or on a ship. For example, a portable trap containing 10^{12} positrons could furnish positrons continuously for ten days at a rate comparable to that of typical radioactive positron sources currently in use (e.g., 10 mCi of ^{22}Na and a solid neon moderator). As noted above, filling a multicell trap with 10^{12} positrons using a typical-strength ^{22}Na source and neon moderator would take several days. However, as indicated above, there are a number of high-flux positron sources, either in operation or under development, which have the capability to fill such a trap in a few hours or less.

The near-term goal of a trap for 10^{12} positrons is likely conservative, and we believe that it has a high probability of success. In the present design, this multicell trap could be made to fit in a volume of only a few cubic meters. It calls for a superconducting magnet and cryogens or a refrigerator. However, one can expect a rapid learning curve associated with the underlying science and technology. It is likely that further improvements in design can be made early in the development of such a multicell device, including increases in storage capacity and confinement time, decreases in the weight and size, and the reduction of other logistical requirements.

ACKNOWLEDGMENTS

We wish to acknowledge J. P. Sullivan and P. Schmidt for their role in the development of the high-field trap used in this work, E. A. Jerzewski for expert technical assistance, and R. G. Greaves for helpful suggestions and critical reading of the manuscript.

This work was supported by the Defense Advanced Research Projects Agency, Grant No. HR0011-05-1-0041, and the National Science Foundation, Grant No. PHY 03-54653.

[1] P. Jean, J. Knodlseder, V. Lonjou, M. Allain, J. P. Roques, G. K. Skinner, B. J. Teegarden, and G. Vedrenne, Astron. Astrophys. **407**, L55 (2003).
[2] C. M. Surko and R. G. Greaves, Phys. Plasmas **11**, 2333 (2004).
[3] M. Amoretti, C. Amsler, G. Bonomi *et al.*, Nature **419**, 456 (2002).
[4] G. Gabrielse, N. Bowden, P. Oxley *et al.*, Phys. Rev. Lett. **89**, 213401 (2002).
[5] P. J. Schultz and K. G. Lynn, Rev. Mod. Phys. **60**, 701 (1988).
[6] See articles in *New Directions in Antimatter Chemistry and Physics*, edited by C. M. Surko and F. A. Gianturco (Kluwer Academic, Dordrecht, 2001).
[7] A. P. Mills, Jr., Nucl. Instrum. Methods Phys. Res. B **192**, 107 (2002).
[8] C. F. Driscoll and J. H. Malmberg, Phys. Rev. Lett. **50**, 167 (1983).
[9] C. F. Driscoll, K. S. Fine, and J. H. Malmberg, Phys. Fluids **29**, 2015 (1986).
[10] T. M. O'Neil, Phys. Fluids **26**, 2128 (1983).
[11] C. M. Surko and T. J. Murphy, Phys. Fluids B **2**, 1372 (1990).
[12] R. G. Greaves and C. M. Surko, Phys. Plasmas **4**, 1528 (1997).
[13] B. M. Jelenkovic, A. S. Newbury, J. Bollinger, W. M. Itano, and T. B. Mitchell, Phys. Rev. A **67**, 063406 (2003).
[14] C. M. Surko and R. G. Greaves, Radiat. Phys. Chem. **68**, 419 (2003).
[15] J. R. Danielson, P. Schmidt, J. P. Sullivan, and C. M. Surko, in *Non-Neutral Plasma Physics V*, edited by M. Schauer, T. Mitchell and R. Nebel (American Institute of Physics, Melville, NY, 2003), p. 149.
[16] O. J. Orient, A. Chutjian, and V. Garkanian, Rev. Sci. Instrum. **68**, 1393 (1997).
[17] E. R. Badman and R. G. Cooks, Anal. Chem. **72**, 3291 (2000).
[18] E. M. Hollmann, F. Anderegg, and C. F. Driscoll, Phys. Plasmas **7**, 2776 (2000).
[19] R. G. Greaves, M. D. Tinkle, and C. M. Surko, Phys. Plasmas **1**, 1439 (1994).
[20] L. V. Jorgensen, M. Amoretti, G. Bonomi, P. D. Bowe, C. Canali, and C. Carraro, Phys. Rev. Lett. **95**, 025002 (2005).
[21] C. M. Surko, R. G. Greaves, and M. Charlton, Hyperfine Interact. **109**, 181 (1997).

[22]C. Hugenschmidt, K. Schreckenbach, M. Stadlbauer, and B. Straßer, Appl. Surf. Sci. **252**, 3098 (2006).
[23]R. Krause-Rehberg, S. Sachert, G. Brauer, A. Rogov, and K. Noack, Appl. Surf. Sci. **252**, 3106 (2006).
[24]H. M. Chen, Y. C. Jean, C. D. Jonah, S. Chemerisov, A. F. Wagner, D. M. Schrader, and A. W. Hunt, Appl. Surf. Sci. **252**, 3159 (2006).
[25]J. R. Danielson and C. M. Surko, Phys. Rev. Lett. **95**, 035001 (2005).
[26]J. R. Danielson and C. M. Surko, Phys. Plasmas **13**, 055706 (2006).
[27]D. L. Eggleston, C. F. Driscoll, B. R. Beck, A. W. Hyatt, and J. H. Malmberg, Phys. Fluids B **4**, 3432 (1992).
[28]B. R. Beck, J. Fajans, and J. H. Malmberg, Phys. Rev. Lett. **68**, 317 (1992).
[29]J. Malmberg, T. M. O'Neil, A. W. Hyatt, and C. F. Driscoll, in *Proceedings of the Sendai Symposium on Plasma Nonlinear Electron Phenomena* (Tohoku University Press, Sendai, Japan, 1984), p. 31.
[30]N. Oshima, T. M. Kojima, M. Niigati, A. Mohri, K. Komaki, and Y. Yamazaki, Phys. Rev. Lett. **93**, 195001 (2004).
[31]R. C. Davidson, *Physics of Nonneutral Plasmas* (Addison-Wesley, Reading, MA, 1990).
[32]K. S. Fine, C. F. Driscoll, and J. H. Malmberg, Phys. Rev. Lett. **63**, 2232 (1989).
[33]C. A. Kapentanokos and A. W. Trivelpiece, J. Appl. Phys. **42**, 4841 (1971).
[34]B. P. Cluggish, Ph.D. thesis, University of California, San Diego, 1995.
[35]J. Fajans, E. Gilson, and L. Friedland, Phys. Rev. Lett. **82**, 4444 (1999).
[36]J. Fajans, E. Gilson, and L. Friedland, Phys. Plasmas **6**, 4497 (1999).
[37]J. Fajans, E. Gilson, and L. Friedland, Phys. Plasmas **8**, 423 (2001).
[38]X. P. Huang, F. Anderegg, E. M. Hollmann, C. F. Driscoll, and T. M. O'Neil, Phys. Rev. Lett. **78**, 875 (1997).
[39]F. Anderegg, E. M. Hollmann, and C. F. Driscoll, Phys. Rev. Lett. **81**, 4875 (1998).
[40]T. M. O'Neil and M. W. Anderson, Bull. Am. Phys. Soc. **51**, 248 (2006).
[41]J. R. Danielson, C. M. Surko, M. W. Anderson, and T. M. O'Neil, Bull. Am. Phys. Soc. **51**, 248 (2006).
[42]R. W. Gould, AIP Conf. Proc. **498**, 170 (1999).
[43]T. M. O'Neil and D. H. E. Dubin, Phys. Plasmas **5**, 2163 (1998).
[44]C. H. Tseng and G. Gabrielse, Hyperfine Interact. **76**, 381 (1993).
[45]R. A. Lewis, G. A. Smith, and S. D. Howe, Hyperfine Interact. **109**, 155 (1997).